Proceedings Paper:

Robinson, G.E.J. orcid.org/0009-0006-9699-1575, Poyraz, O., Sims, N.D. et al. (1 more author) (2025) A model for chatter stability enhancement through lattice support structures. In: Ducobu, F. and Lauwers, B., (eds.) Procedia CIRP. 20th CIRP Conference on Modeling of Machining Operations, 22-23 May 2025, Mons, Belgium. Elsevier BV , pp. 525-530.

https://doi.org/10.1016/j.procir.2025.02.090

Available online at www.sciencedirect.com

ScienceDirect

Procedia CIRP 133 (2025) 525–530

www.elsevier.com/locate/procedia

20th CIRP Conference on Modeling of Machining Operations

A model for chatter stability enhancement through lattice support structures

George E.J. Robinson *,a, Ozgur Poyraz[c], Neil D Sims[b], Pete Crawforth[a]

[a]Advanced Manufacturing Research Centre, The University of Sheffield, Catcliffe, Rotherham, S60 5TZ
[b]School of Mechanical Aerospace and Civil Engineering, The University of Sheffield, Mappin Street, Sheffield S1 3JD, UK
[c]Advanced Manufacturing Research Centre North West, The University of Sheffield, Blackburn BB2 7HP, UK

* Corresponding author. *E-mail address:* grobinson3@sheffield.ac.uk

Abstract

The machining of near net shapes (NNS) produced by laser powder bed fusion (L-PBF) presents challenges regarding the stiffness of components. Notably, complex geometries featuring thin-walled, slender and hollow regions are of particular interest to additive manufacturing technologies, yet to meet the dimensional and surface quality requirements of functional parts, machining is often deemed necessary. Compliant regions of a workpiece are prone to chatter, and workholding becomes difficult with complex surfaces. Previous works have explored the pure stiffening of flexible workpieces with solid elements such as buttresses and lateral stiffeners. Meanwhile, advances have been made in mesostructural design for a range of metamaterial functions due to the maturation of L-PBF.

Building upon these two concepts, the present contribution investigates what damping and stiffening effects a lattice support structure would have on the chatter stability of a flexible workpiece produced by L-PBF. A dynamic model of a cantilever beam supported by a spring and a viscous damper is proposed to predict the vibrational behaviour of a workpiece supported by a lattice support structure. A preliminary modal test is carried out to acquire damping behaviour to inform the model, and provide a deeper understanding of the relationships between lattice parameters and damping.

This study is part of an ongoing discussion into the post-processing of NNS parts produced by L-PBF. It presents the concept of additive design for machining, and prompts investigation into how a mesostructural support could be designed to enhance machining operations. As the proposed structure is an addition to the functional part, it should be sacrificial, and to be sacrificial it should be removed effectively and efficiently. The present contribution seeks to provoke a discussion around these emerging concepts.

Keywords: Milling; Lattice; Additive Manufacturing; Workholding

1. Introduction

The geometrical flexibility afforded by laser-powder bed fusion (L-PBF) presents significant potential for innovative design, particularly in creating lightweight structures, offering the conservation of material when compared to subtractive methods. However, due to multiple reasons such as surface roughness [1] and dimensional inaccuracy, machining is often a necessary step in the post-processing of an additively produced component.

One challenging aspect of the machining of slender near-net components is the structural flexibility of the unfinished form, making them prone to deflection and vibration. When conventional methods of fixturing are used, complex planning and manual intervention is often required. In the case of L-PBF, this results in the design of custom fixturing [2], hindering the rapid production cycle and design freedom that L-PBF benefits from. Similarly, many traditional methods of passive damping such as tuned mass dampers [3] can be relatively bulky, require installation prior to machining and rely on narrowband attenuation.

Sacrificial support structures have often been employed in the machining of parts from-billet or components built via directed energy deposition [4]. The objective of the structures is to allow stable machining through increasing the minimum stiffness of the workpiece and sufficiently supporting the workpiece against the expected machining forces. These structures take the form of solid buttresses supporting thin walls. Schmitz [5] employs a static stiffness-based design strategy for ramp and step shaped preforms supporting thin walls, demonstrating a framework for optimising material deposition with respect to total

10.1016/j.procir.2025.02.090

cost. Didier et al [6] considers the suspension of the workpiece from the additive build plate with a lattice, using the supporting structure as a clamping device for the workpiece. Some fixtures have been developed [7] which incorporate lattice elements to dissipate vibrations. The present contribution considers that a supporting structure can be designed to increase the passive damping of the workpiece as well as stiffening and resisting machining forces.

The design of mesostructures, such as lattices and triply periodic minimal surfaces, has garnered an increased research focus with the advancement of AM methods. In particular, the design of metamaterials has been of interest, as they are designed to outperform the constituent, conventional material for a target property. A well documented instance is that of the body centred cubic (BCC) lattice [8], which outperforms the equivalent stiffness to mass ratio of the solid, constituent material. Similarly, superior damping properties have been recorded in lattice structures. Scalzo et al. [9] explored the relationship between lattice scale and damping, and described the correlation with a scale-dependent Rayleigh damping model, linking a reduction in cell size to an increase in damping. Mesostructures designed to exhibit damping behaviour well beyond that of the constituent bulk material, could be considered metamaterials designed for damping.

The damping mechanisms within L-PBF mesostructures are little understood, however insights can be drawn from works investigating the behaviour of metallic foams [10]. The cited study proposes that the enhanced damping effect observed in porous metallic structures is attributed to high multiaxial stress concentrations that occur within the cell, inducing viscous-like sliding of atoms relative to each other. This mechanism correlates with a trend where metallic foams of lower relative densities show increased damping capacity due to more pronounced local deformation, leading to energy dissipation mechanisms that are absent in bulk materials.

Rosa et al. [11] proposed that the presence of cracks within L-PBF lattice structures are responsible for a frictional contribution to damping due to the relative movement between the surfaces of the crack. Typically, this would disqualify the use of such structures in applications subjected to high cyclic loading, however the unique nature of sacrificial preforms is such that it is tolerant of crack propagation. Specifically, in the case suggested by the present work, the preforms are for temporary use under low-cycle conditions, so fatigue does not jeopardise the functionality of the final component.

The modelling of mesostructures by conventional structural methods such as finite element method, presents significant challenges and imposes a high computational burden [12]. Specifically, surface-to-volume ratios of the structures are orders of magnitude higher than that of typical geometries.

Therefore, developing a model and establishing a methodology for assessing the performance of a mesostructures support is an important step in developing metadamped sacrificial preforms for enhancing machining stability for the post-processing of L-PBF workpieces. The present study seeks to address this research gap through a preliminary experimental and numerical analysis that will ultimately enable the expediated evaluation of future designs.

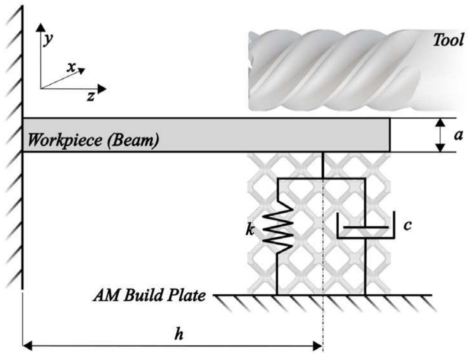

Fig. 1. Composite schematic of the machining operation simulated by the dynamic model

2. Model development

To support experimental analysis in future investigations, simulations should be employed to deepen the understanding of process dynamics and validated through experimental results to identify discrepancies between predicted and observed behaviours.

In the present study, a hybrid model was developed to characterise the support structure and predict chatter stability. A thin-wall machining scenario was deemed as an appropriate representative case to ensure that the dynamics of the workpiece predominantly govern the process, allowing the spindle and tool to be considered comparatively rigid.

The modelled process is illustrated in Fig. 1. A 100 mm (h) solid wall, of depth 60 mm, thickness (a) of 5 mm composes the workpiece. A region of 60 x 20 mm (x x z) at the upper tip of the wall is supported by a BCC lattice. The support extends to 500 mm in the y direction. The supporting BCC lattice is supported by a rigid wall on the opposing side. To simplify boundary conditions, the thin wall is assumed as encastre to the rest of the rigid workpiece. In practice, this approach corresponds to retaining the workpiece (including support structure) on the additive build plate, which effectively welds the workpiece to the AM build plate. This setup would enable the implementation of more robust clamping arrangements on the plate.

The lattice parameters varied are cell size and volume fraction, as shown in Fig. 2. It has been well established [13] that the volume fraction of a cellular structure has a power law relationship with the effective elastic modulus. This leads to the idealisation that for a given geometry, both BCC-4-0.7 and BCC-10-1.75 designs of constant volume fraction 0.1484, should exhibit the same effective stiffness. Likewise, samples BCC-4-1.4 and BCC-10-3.5 of volume fraction 0.5212 should exhibit the same, increased effective stiffness. The lattice cells were designed with fillets of constant radii at each strut intersection, and the fillet is scaled with the cell to be half of the strut diameter. The strut diameters are selected such that they are at the extremes of reliable, unsupported buildability. A minimum strut diameter of 0.7 mm ensures struts are solid and defects do not

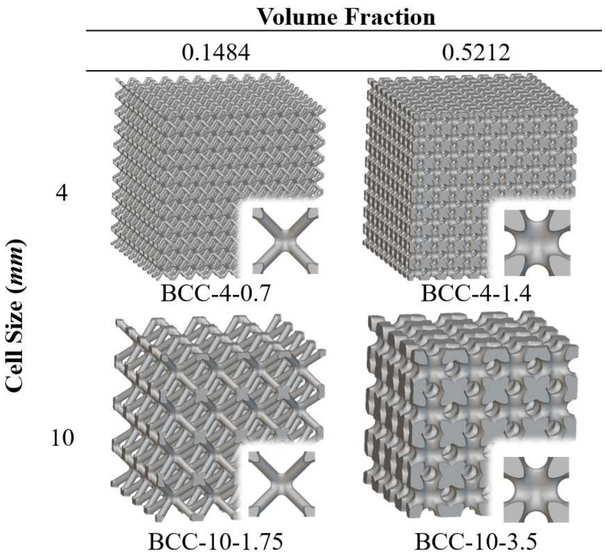

Fig. 2. Renders of 40 x 40 x 40 mm representative regions of lattice variations and corresponding sample names. Sample name AAA-B-CC corresponds to AAA: lattice type, B: cell size mm, C: Strut diameter mm

split struts, and a maximum strut diameter of 3.5 mm ensures that unsupported arches are less than 4 mm in diameter allowing for unsupported build. Cell sizes are selected such that full cells fit within the 60 x 20 mm support region of the machining samples, to avoid the truncation of cells. M300 maraging steel was selected for this study, primarily due to its availability for use in L-PBF platforms and its established machinability.

It is recognised that the additively built maraging steels, like most additively processed metals, exhibit anisotropy due to the complex thermal cycles involved in the layer-by-layer build process [14]. Rapid heating, cooling and reheating leads to a bias in microstructural textures across build orientations which results in anisotropy in elastic modulus and other properties. This material anisotropy is factored into the model in this study. However, it will be assumed that the material properties are homogenous, regardless of geometry. This assumption simplifies analysis but overlooks the difference in the bulk properties between the material comprising the thin wall and the support structure.

2.1. Metamaterial modelling

The complex geometries inherent to lattice structures present a significant challenge when attempting to model their behaviour. A common method of representing such structures is through a homogenisation technique [15, 13], treating the mesostructure as a metamaterial. A representative elementary volume (REV) is selected, which encapsulates the desired characteristics of the lattice. The REV is analysed using finite element methods (FEM) to determine the effective material properties. In this case, it is the anisotropic stiffness tensor which is desired.

The homogenised properties can then be applied to the macro-scale without the computational burden of discretising a large and complex model. This approach balances accuracy and computational efficiency, as the need to model the entire macro-scale geometry is bypassed. However, care must be taken to ensure the REV accurately captures the behaviour of the lattice. In particular, edge effects should be avoided and boundary conditions should reflect actual constraints.

As defined by Hill [16], the representative volume should be structurally typical of the overall macroscopic volume, containing sufficient inclusions such that the apparent moduli are independent of the surface of forces and displacements. To satisfy this criterion, a volume consisting of 4 x 4 x 4 unit cells was analysed.

The BCC unit cells were designed parametrically using boundary-representation (b-rep) CAD software, Fusion360, and tessellated with implicit modelling software, nTop. A voxel-based meshing method was employed in nTop for the REVs, allowing for a fine mesh with consistent quadratic tetrahedral elements while maintaining geometric accuracy and computational efficiency. The meshed geometry was then exported from nTop and imported into ANSYS before being analysed using the FEM in ANSYS, conducting static mechanical assessments to evaluate the structural performance.

The elastic moduli of the AM maraging steel are acquired from a reference in literature [14]. The reference uniaxially tested ASTM E8M standard dog-bone samples built at 0°, 45°, and 90°orientations to the build plate. The uniaxial compression of the REVs is set up by applying a fixed support at the negative end of the axis being analysed, with a compressive displacement applied to the positive side. Displacement in directions that are not the axis being tested are constrained at the boundaries of the REV. A time step of 1 s and a total simulation of 10 s is used, with a maximum displacement of $\frac{1}{10}$ the REV size. Since the focus is on small displacements of the support structure during machining, only the elastic region of the stress-strain curve is relevant. To ensure this condition is met, the simulation avoids entering the densification stage of the lattice compression and excludes plastic deformation at the joints within the lattice.

The effective elastic modulus of the REV was obtained through the strain energy method, by taking the total strain energy of the REV under compression and applying Hooke's law. The mean elastic modulus is taken across all simulation intervals. Values of elastic modulus in x, y and z comprise the C11, C22 and C33 components of the anisotropic stiffness tensor respectively. Similarly, the uniaxial shear of the REVs is set up with a fixed support at the negative end but with a fixed, steady ramped force at the opposing end. Care is taken to select a force in each scenario to avoid large deformations. The effective shear modulus is obtained through the engineering strain energy method. Values of shear modulus in xy, xz, and yz comprise the C44, C55, and C66 components of the anisotropic stiffness tensor respectively.

2.2. Damping representation

A representation of the damping behaviour of the support structure is integral to the modelling of the process to account for energy dissipation during machining. A free-free modal test was deemed appropriate to obtain values for damping for each

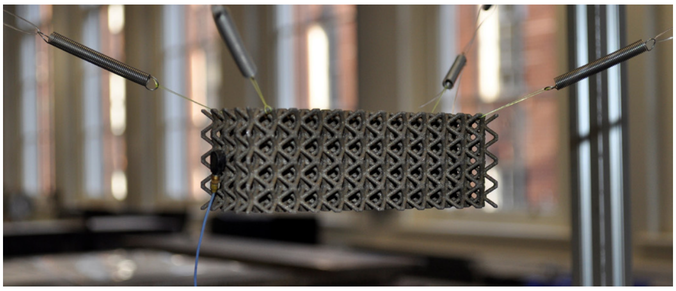

Fig. 3. Experimental setup of the free-free modal testing of the BCC-10-1.75 sample

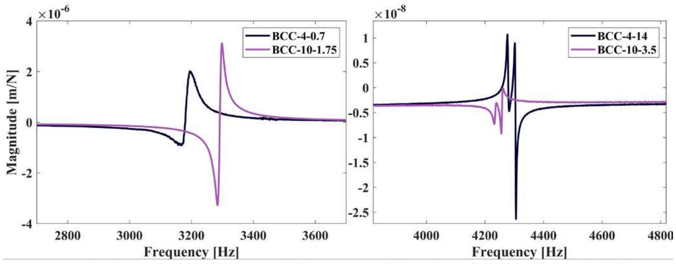

a) Lattices of volume fraction 0.1484 b) Lattices of volume fraction 0.5212

Fig. 4. Receptance magnitude plots obtained from the free-free modal testing

Table 1. Modal parameters for the extension mode extracted via the curve fit method

Lattice	ω_n (Hz)	ζ	k (MN/m)	β (μ s)
BCC-4-0.7	3180	0.0048	36.4	3.0187
BCC-10-1.4	3291	0.0020	40.6	1.215

lattice case. Large samples of 120 x 40 x 40 mm were built via L-PBF with a laser power of 200 W, scan speed of 1000 mm/s, particle size distribution between 15 - 53 μm, and hatch overlap of 70 μm on an Aconity MIDI platform. Each sample was suspended from lightweight line and springs, as shown in Fig. 3.

As the support structure acts predominantly in compression, the extension mode is the focus of analysis. To effectively excite the extension mode, the accelerometer is bonded with wax to one end of the long (120 mm) axis, while the hammer applies excitation to the opposing end. This arrangement enables a more accurate characterisation of the mode relevant to the performance of the support structure. Multiple impact measurements were taken and the resulting receptance is plotted in Fig. 4. Samples BCC-4-0.7 and BCC-10-1.75 both show a dominant resonant peak, with sample BCC-4-0.7 exhibiting greater damping. Single degree of freedom modal parameters are extracted through the curve fit method and displayed in Table 1. A simplified Rayleigh damping model was adopted to approximate the modal damping for the support geometry simulated in the dynamic model.

$$\beta \approx \frac{c}{k} = \frac{2\zeta}{\omega_n} \tag{1}$$

The Rayleigh coefficient (β, in s) allows for the scaling of modal damping (c in s$^-$1) in proportion to modal stiffness (k in N/m), enabling an approximation of the damping ratio across different metamaterial macro-geometries [9]. Where ζ is damping ratio, and ω_n is the natural frequency in Hz. Samples BCC-4-1.4 and BCC-10-3.5 (Fig. 4b) both exhibit a double resonance at the extension mode, suggesting a more complex dynamic behaviour. Consequently, the Rayleigh model is deemed unsuitable for these cases as a damping ratio for a single peak cannot be obtained. These structures are excluded from further modelling.

2.3. Dynamic model

A dynamic model for the frequency response of the supported flexible wall was developed. The wall assumes the form of a cantilever beam, as depicted in Fig. 1, with a spring-damper support acting at the beam tip. The following general assumptions are made:

1. The beam is uniform along the span (z-direction).
2. The beam is composed of a homogenous isotropic material.
3. Only deformations normal (y-direction) to the undeformed beam axis are considered.
4. The shear centre of the beam coincides with the centre of mass.
5. The amplitudes of vibration are relatively small in comparison to the length of the beam.

The transverse deformation of the beam is the sum of flexure and shear deformations, and will be estimated using the Southwell-Dunkerley approximation:

$$\frac{1}{\omega_n^2} = \frac{1}{\omega_F^2} + \frac{1}{\omega_S^2} \tag{2}$$

Where ω_n is the fundamental natural frequency of the beam, ω_F is the fundamental frequency as predicted by flexure theory, and ω_S is as predicted via shear theory. The flexure beam theory follows the relationships computed by Maurizi et al. [17], which results in the following formula for the fundamental natural frequency in Hertz:

$$\omega_F = \frac{\lambda_F^2}{2\pi l_b^2}\sqrt{\frac{EI_{xx}}{m}} \tag{3}$$

Where m is mass per unit length in kg/m, and λ_F is the nontrivial solution to the transcendental frequency equation solved by Maurizi et al. and is a function of support stiffness and beam stiffness. l_b, w_b, and h_b is the length, width and height of the beam in the z, x and y directions respectively, in m. E is the Young's modulus of the beam material in Pa, and I_{xx} is the second moment of inertia with respect to the x axis in m^4. The shear theory follows the approach laid out by Blevins [18]. Considering shear deformation results the following formula for fundamental natural frequency in Hertz:

$$\omega_S = \frac{\lambda_S}{2\pi l_b}\sqrt{\frac{EI_{yy}}{m}} \tag{4}$$

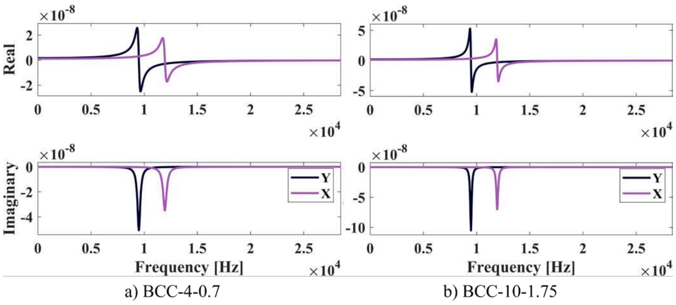

Fig. 5. Real and imaginary components of the generated receptance plot of the x and y bending modes of the flexible wall supported by BCC-4-0.7 and BCC-10-1.75 lattices

λ_S is the non-trivial solution to the transcendental frequency equation:

$$\cot(\lambda_S) = -\frac{kl_b}{Kw_bh_bG\lambda_S} \tag{5}$$

Where G is the shear modulus of the beam material in Pa, K is the shear coefficient for a rectangular beam. The fundamental frequencies in both x and y directions are calculated, and care is taken to ensure they are separate and the bending mode of the beam in y (normal to feed direction) is dominant. The support stiffnesses in y (k_y) and x (k_x) directions are calculated by Eq.6 and Eq. 7 respectively:

$$k_y = \frac{C_{33}w_sl_s}{h_s} \tag{6}$$

$$k_x = \frac{C_{66}w_sl_s}{h_s} \tag{7}$$

Where C_{33} and C_{66} are the components of the anisotropic stiffness tensor as acquired through the method described in Section 2.1.Where l_s w_s, and h_s are the length, width and height of the support structure in the z, x, and y directions respectively.

Using the Southwell-Dunkerly approximation to estimate the fundamental frequency (ω_n) and the Rayleigh approximation (Eq.1) to scale the damping ratio (ζ) based on the metamaterial stiffness profiles obtained through FEM, the FRFs are formulated for both lattice parameter variations. The real and imaginary components of these FRFs are computed with Eq. 8, and Eq. 9, respectively. The FRFs are plotted in Fig. 5, illustrating the dynamic response for both lattice parameter variations.

$$Im(FRF) = \frac{1}{k}\frac{-2\zeta\frac{\omega}{\omega_n}}{(1-\frac{\omega}{\omega_n})^2 + (2\zeta\frac{\omega}{\omega_n})^2} \tag{8}$$

$$Re(FRF) = \frac{1}{k}\frac{(1-\frac{\omega}{\omega_n})^2}{(1-\frac{\omega}{\omega_n})^2 + (2\zeta\frac{\omega}{\omega_n})^2} \tag{9}$$

2.4. *Stability lobe plotting*

To provide a comparative demonstration of the machining stability modification of the workpiece when supported by a damping mesostructure, the stability lobe diagram of the system using an example tool is plotted. The Fourier series approach to SLD plotting is taken as founded by Altintas and Budak [19].

For the purpose of demonstration, a tool of diameter 16 mm with 5 flutes, and a radial engagement of 2 mm. Cutting force coefficients are provided as $K_t = 700$ MPa and $K_n = 210/K_t$ MPa .

The method begins by calculating the oriented FRF from the FRFs in the x and y directions, under the assumption of no cross-talk between responses due to the orthogonality of these directions, and the assumption of a linear response. As the focus of the study is on the workpiece dynamic response, the tool is assumed to be rigid, and the frequency response of the tool is neglected. This assumption results in a significantly higher limiting depth of cut compared to scenarios where tool dynamics are considered. Regardless, the generated plots effectively demonstrate the stability enhancement achieved through the modification of lattice support parameters. The SLDs are plotted in Fig. 6.

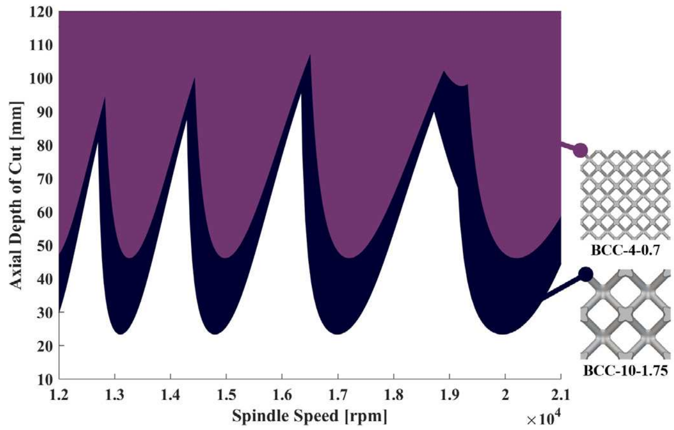

Fig. 6. SLDs of the flexible wall workpiece as supported by lattices BCC-4-0.7 and BCC-10-1.75

3. Discussion of results

It has been observed that for a comparable stiffness, the BCC-4-0.7 lattice shows a significant increase in damping capacity when compared to the BCC-10-1.75 lattice of same volume fraction. This supports hypotheses observed in literature, linking a reduced cell scale to an increase in damping. This increase in damping has a significant effect on the cutting stability as illustrated by the SLD, greatly increasing the limiting depth of cut (97.5% increase) when utilising the BCC-4-0.7 lattice over the BCC-10-1.75 lattice. A valuable consideration when applying such lattices as a sacrificial support structure in machining, given that both consume the same amount of material, and exhibit the same effective stiffness. Both support structures greatly increase the limiting depth of cut, from 0.109 mm in the unsupported case, to 23.42 mm when supported with the BCC-10-1.75, to 46.22 mm when supported by the BCC-4-0.7 lattice.

The same observation could not be made for the BCC-4-1.4 and BCC-10-3.5 samples, which exhibited a double resonance mode. This behaviour suggests that these structures may be transitioning from behaving like conventional lattices to func-

Table A.2. C_{33} and C_{66} of the anisotropic stiffness tensors obtained for the lattices through the method described in 2.1

Lattice	C_{33} (GPa)	C_{66} (GPa)
BCC-4-0.7	1.37	0.900
BCC-10-1.75	1.37	0.906
BCC-4-1.4	37.8	9.77
BCC-10-3.5	37.8	9.80

tioning more like solids with periodic porosity. Consequently, damping mechanisms typically associated with lattices, such as localised microplasticity, may not apply to these configurations. As a result, these structures were deemed unsuitable for further integration into the flexible workpiece model, as the Rayleigh approximation is not valid in this context. The precise mechanics underlying the dynamic behaviour of these lattices remain unclear and warrant further investigation.

4. Conclusions and future direction

In the present contribution, a model and a method for assessing the potential machining stability enhancement of a metamaterial support structure was presented. The model accounts for the material anisotropy inherent to the additive process, and is replicable for a range of materials and support structure geometries. This versatility increases the efficiency and accessibility of experimental analysis for future research, allowing for rapid assessment of different support structures.

A relationship between reduced cell size and increased damping was identified, providing a deeper insight into the mechanisms driving energy dissipation in lattice structures. This is potentially due to an increased number of nodes within the cell, offering sites for localised stress concentrations. The reduced scale increases the likelihood of occurrence of process-induced defects, leading to severed or undersized struts within the lattice structure. These defects create points of relative movement between adjacent surfaces at the fracture sites, which could contribute to energy dissipation through frictional interactions.

The concept of mesostructural support systems along with on-build-plate machining, has been explored in this study, demonstrating the versatility of additive-subtractive manufacturing. This approach reduces the need for specialised fixturing and extensive manual intervention. These supports can be integrated into the build,to create stiff and dampened near-net forms.

Acknowledgements

This research was funded by the EPSRC. The authors wish to gratefully acknowledge support provided by the members of The University of Sheffield Advanced Manufacturing Research Centre.

Appendix A. Anisotropic stiffness tensors

References

[1] Maleki, E., Bagherifard, S., Bandini, M., Guagliano, M., 2021. Surface post-treatments for metal additive manufacturing: Progress, challenges, and opportunities. Additive Manufacturing 37, 101619.
[2] Schuh, G., Bergweiler, G., Lichtenthäler, K., Fiedler, F., Puente Rebollo, S. de la, 2020. Topology Optimisation and Metal Based Additive Manufacturing of Welding Jig Elements. Procedia CIRP, 53rd CIRP Conference on Manufacturing Systems 2020 93, 62–67.
[3] Bolsunovsky, S., Vermel, V., Gubanov, G., Leontiev, A., 2013. Reduction of Flexible Workpiece Vibrations with Dynamic Support Realized as Tuned Mass Damper. Procedia CIRP 8, 230–234.
[4] Vaughan, D., Saldana, C., Kurfess, T., Nycz, A., 2022. Implementation of Sacrificial Support Structures for Hybrid Manufacturing of Thin Walls. Journal of Manufacturing and Materials Processing 6.
[5] Schmitz, T., Corson, G., Olvera, D., Tyler, C., Smith, S., 2023. A framework for hybrid manufacturing cost minimization and preform design. CIRP Annals 72, 373–376.
[6] Didier,P.,Le Coz,G.,Robin,G.,Lohmuller,P.,Piotrowski,B.,Moufki, A., Laheurte,P.,2021. Consideration of SLM additive manufacturing supports on the stability of flexible structures in finish milling. Journal of Manufacturing Processes 62, 213–220.
[7] Picavea,J.,Mohammad,A.,Gameros,A., Yang, J., Axinte, D., 2023. Synergistic integration of vibration absorption and damping into 3D-printed fixtures for thin-wall machining. CIRP Annals 72, 357–360.
[8] Ushijima, K., Cantwell, W.J., Chen, D.H., 2013. Prediction of the mechanical properties of micro-lattice structures subjected to multi-axial loading. International Journal of Mechanical Sciences 68, 47–55.
[9] Scalzo, F., Totis, G., Vaglio, E., Sortino, M., 2020. Experimental study on the high-damping properties of metallic lattice structures obtained from SLM.
[10] Banhart, J., Baumeister, J., Weber, M., 1996. Damping properties of aluminium foams. Materials Science and Engineering: A 205, 221–228.
[11] Rosa, F., Manzoni, S., Casati, R., 2018. Damping behavior of 316L lattice structures produced by Selective Laser Melting. Materials & Design 160, 1010–1018.
[12] Kanit, T., Forest, S., Galliet, I., Mounoury, V., Jeulin, D., 2003. Determination of the size of the representative volume element for random composites: Statistical and numerical approach. International Journal of Solids and Structures 40, 3647–3679.
[13] Gibson, L.J., Ashby, M.F., 1997. Cellular Solids: Structure and Properties. Cambridge University Press.
[14] Mooney, B., Kourousis, K.I., Raghavendra, R., 2019. Plastic anisotropy of additively manufactured maraging steel: Influence of the build orientation and heat treatments. Additive Manufacturing 25, 19–31.
[15] Kanit, T., Forest, S., Galliet, I., Mounoury, V., Jeulin, D., 2003. Determination of the size of the representative volume element for random composites: Statistical and numerical approach. International Journal of Solids and Structures 40, 3647–3679.
[16] Hill, R., 1963. Elastic properties of reinforced solids: Some theoretical principles. Journal of the Mechanics and Physics of Solids 11, 357–372.
[17] Maurizi, M.J., Rossi, R.E., Reyes, J.A., 1976. Vibration frequencies for a uniform beam with one end spring-hinged and subjected to a translational restraint at the other end. Journal of Sound and Vibration 48, 565–568.
[18] Blevins, R.D., 1979. Formulas for natural frequency and mode shape. New York: Van Nostrand Reinhold Co.
[19] Altintaş, Y., Budak, E., 1995. Analytical Prediction of Stability Lobes in Milling. CIRP Annals 44, 357–362.